

Distribution of the extensive Doppler redshift of quasars

Yi-Ping Qin^{1,2}, Hong-Tao Liu^{1,3}, En-Wei Liang^{1,2}, Yun-Ming Dong^{1,3} and

Cheng-Yue Su^{1,3,4}

¹National Astronomical Observatories/Yunnan Observatory, Chinese Academy of Sciences, P. O. Box 110, Kunming, Yunnan, 650011, P. R. China

²Physics Department, Guangxi University, Nanning, Guangxi, 530004, P. R. China

³ The Graduate School of the Chinese Academy of Sciences

⁴ Department of Physics, Guangdong Industrial University, Guangzhou, Guangdong, 510643, P. R. China

Abstract

We make an analysis of the distribution of the extensive Doppler redshift defined as $\tilde{z}_{Dopp} = (z_{abs} - z_{em})/(1 + z_{em})$ with a sample of 1317 absorption redshifts available from 401 quasars. The analysis reveals a bi-peak structure in the distribution, with one component located at $\tilde{z}_{Dopp} \simeq 0.00$ and the other at $\tilde{z}_{Dopp} \simeq -0.01$. A study of some possible causes suggests that the structure can be well interpreted: while the absorbers inside the same cluster as the quasar concerned could contribute to the first component and the less populated space between clusters could explain the gap between the two peaks, the typical distance between clusters could account for the second component. If the bi-peak structure is true, which needs to be confirmed by complete samples, one would be able to obtain some useful cosmological information.

Key words: cosmology: observations — galaxies: distances and redshifts — quasars: absorption lines — quasars: emission lines

1 Introduction

Emission redshifts of quasars are believed to be of cosmological origin. Absorption redshifts of the objects must be produced by the absorbers in front of them along the line of sight. In fact, the Lyman-limit systems (Tytler 1982) are clearly due to intervening gas that is unassociated with the

quasars since they usually appear at redshifts significantly less than the corresponding emission redshifts. The damped Ly α systems observed in quasars are thought to arise on sight lines which pass through galactic disks. Generally, absorption lines of quasars are supposed to arise in material directly associated with galaxies, such as dark halos.

As emphasized by Peterson (1997), at least two absorption lines are required for an unambiguous identification and redshift measurement. The most commonly detected absorption lines are Ly α λ 1216, CIV λ 1548, 1551, and MgII λ 2795, 2802. Other lines that are commonly detected include CII λ 1335, SiIV λ 1394, 1403, MgI λ 2852, and several UV resonance lines of FeII.

Obviously, absorption redshifts of quasars can be due to both the cosmological distance and the Doppler motion of absorbers. Broad absorption features are detected in the shortward wings of resonance lines of some quasars (Weymann et al. 1981). The absorption is always at wavelengths shortward of line center, which indicates that the absorbing gas is flowing outward from the nucleus, and the high ionization level and high outflow velocities of the gas strongly suggest that the corresponding absorbers are closely associated with the nuclear regions. As mentioned in Peterson (1997), an absorption-line system consists of a number of absorption lines in a quasar spectrum that are all at very nearly the same redshift z_{abs} and presumably arise in the same absorber. The redshift of these absorption lines will reflect the cosmological distance of the absorbing cloud rather than that of the quasar which will have emission redshift z_{em} . It is expected that quasar spectra will show absorption lines characterized by $z_{abs} < z_{em}$. In most cases this is true (see e.g., Junkkarinen, Hewitt, and Burbidge 1991; Hewitt and Burbidge 1993; Qin et al. 2000). Some absorption lines are detected at redshifts slightly larger than z_{em} (see e.g., Weymann et al. 1977; Qin et al. 2000). The $z_{abs} > z_{em}$ phenomenon is thought to be attributable to some combination of quasars and the absorber peculiar velocities relative to the Hubble expansion and intrinsic wavelength shifts of the broad absorption lines relative to their systemic redshifts (Gaskell 1982).

The number of absorption lines we expect along a line of sight to a quasar is given by $dN(z) = n(z)\sigma(z)dl(z)$, where $n(z)$ is the number density of absorbers at z , $\sigma(z)$ is their cross-section for producing absorption lines, and $dl(z)$ is an element of proper path length (see Peterson 1997). This number can reveal evolution in comoving density or cross-section of absorbers (see e.g., Sargent et al. 1988). Here, we study another aspect of the absorption feature of quasars, the distribution of the so-called extensive Doppler redshift which is a relative absorption redshift defined relative to

the corresponding emission redshift. We will try to find out any cosmological information implied by this distribution.

We present the definition of the extensive Doppler redshift in section 2. The distribution of the extensive Doppler redshift for a sample of quasars is presented in section 3. Possible interpretation of the distribution is discussed in section 4. Conclusions are given in section 5.

2 Definition of the extensive Doppler redshift

As mentioned above, absorption redshifts, z_{abs} , of quasars reflect both the Doppler motion and the cosmological distance of the absorbers. When z_{abs} is very close to the corresponding emission redshift, z_{em} , the absorber must be associated with the same host galaxy and the difference between the two redshifts must be produced by the Doppler motion of the absorber. If z_{abs} is significantly less than the corresponding emission redshift, the Doppler motion alone would not be able to account for the difference between the two. Instead, the main part of that difference would probably be due to distance between the absorber and the host galaxy concerned (in other words, the absorber would be that associated with another galaxy). Assuming the absorber and the quasar are associated with the same host galaxy, the quasar is stationary relative to the cosmological frame, and the difference between the absorption redshift and the emission redshift is due to the Doppler motion of the absorber relative to the quasar, then the Doppler redshift related to the motion is (Kembhavi and Narlikar 1999)

$$\tilde{z}_{Dopp} = \frac{z_{abs} - z_{em}}{1 + z_{em}}. \quad (1)$$

We take this equation as the definition of \tilde{z}_{Dopp} and apply it to all absorption redshifts of quasars. The quantity \tilde{z}_{Dopp} is called an extensive Doppler redshift.

Obviously, when z_{abs} is significantly less than z_{em} , \tilde{z}_{Dopp} is no more an element reflecting Doppler motions. Instead, it might become a cosmological quantity. Assuming both z_{abs} and z_{em} arise from cosmological distances, in terms of the scale factor of the universe $R(t)$ we come to

$$\tilde{z}_{Dopp} = \frac{R(t_{em})}{R(t_{abs})} - 1. \quad (2)$$

In this situation, \tilde{z}_{Dopp} becomes in some sense a relative redshift between the quasar and the absorber.

Generally, for quasars with $z_{abs} < z_{em}$, one can define a relative redshift z_{ae} between the quasar and the absorber as

$$1 + z_{ae} = \frac{R(t_{abs})}{R(t_{em})} = \frac{1}{1 + \tilde{z}_{Dopp}}, \quad (3)$$

with the last equality following from the definitions given above. In terms of the emission and absorption redshifts the expression of z_{ae} is

$$z_{ae} = \frac{z_{em} - z_{abs}}{1 + z_{abs}}. \quad (4)$$

When taking $t_{abs} = t_0$ we get $1 + z_{ae} = 1 + z_{em}$ and $1 + \tilde{z}_{Dopp} = (1 + z_{em})^{-1}$, suggesting that, while z_{ae} is a conventionally defined redshift, \tilde{z}_{Dopp} is an inversely defined one. When $|\tilde{z}_{Dopp}| \ll 1$ we come to $z_{ae} \simeq -\tilde{z}_{Dopp}$. It shows that, when z_{ae} and \tilde{z}_{Dopp} act as Doppler redshifts (in the case when z_{abs} and z_{em} are very close, e.g., when the absorber is inside the same host galaxy of the quasar), $z_{ae} > 0$ (while $\tilde{z}_{Dopp} < 0$) suggests that the absorber moves towards the quasar, and $\tilde{z}_{Dopp} > 0$ (while $z_{ae} < 0$) corresponds to the situation when the absorber moves away from the quasar. [One can find from (4) that, in the case of $z_{abs} \simeq z_{em}$, z_{ae} comes to be a Doppler redshift of the quasar relative to the absorber.]

3 Distribution of the redshift

It is understood that a small value of \tilde{z}_{Dopp} would reflect a real Doppler redshift relative to the quasar while a large value of \tilde{z}_{Dopp} would correspond to the case when the absorber is associated with another galaxy and hence the difference between the absorption redshift and the corresponding emission redshift would mainly be due to the cosmological distance between the two galaxies. If we believe that the majority of the absorbers of quasars are objects associated with galaxies, then we can expect a gap in the distribution of \tilde{z}_{Dopp} due to the vast distance between galaxies or clusters. If so, one might probably be able to draw some useful cosmological information from this gap. In the following we employ a large sample of absorption redshifts to make the distribution analysis.

In the catalogue of Hewitt and Burbidge (1993), there are 401 quasars with both of their absorption and emission redshifts available. For these 401 quasars, where emission redshifts range from 0.158 to 4.733, the number of absorption redshifts in total is 1317. We calculate the extensive Doppler redshift following (1), where both the absorption and emission redshifts are taken from the same source, and obtain 1317 extensive Doppler redshifts.

The distribution of the extensive Doppler redshift of the sample is shown in Fig. 1. As is expected, displayed in the figure, there indeed exists a gap in the vicinity of the origin. Associated with the gap, there stands a bi-peak structure with one component located at $\tilde{z}_{Dopp} \simeq 0.00$ and the other at $\tilde{z}_{Dopp} \simeq -0.01$.

4 Cosmological implication of the distribution

As mentioned above, the extensive Doppler redshift could arise from the relative velocity between the absorber and the quasar or the distance between them. Let us investigate if the bi-peak structure can be produced by the distribution of Doppler velocities of galaxies. This can straightforwardly be done when a distribution of Doppler velocities of galaxies is studied.

We employ a large number (544) of proper velocities of galaxies in the Mark III Catalog of Galaxy Peculiar Velocities (Willick et al. 1997). With these velocities, we can calculate the corresponding Doppler redshifts by

$$z_{Dopp} = v/c, \quad (5)$$

where c is the speed of light. In deriving this formula, the condition of $v/c \ll 1$ is assumed. The distribution of z_{Dopp} derived from these proper velocities is shown in Fig. 2. Displayed in the figure we find that the distribution of these Doppler redshifts peaks at $z_{Dopp} \simeq -4.8 \times 10^{-4}$. This value is obviously very much smaller in magnitude than the second component, $\tilde{z}_{Dopp} \simeq -0.01$, in Fig. 1. Hence, the assumption that the second component arises from the distribution of galaxy velocities would not be true. Instead, it might probably be due to cosmological distances between the absorbers and their corresponding quasars.

It is noticed that the peculiar galaxy velocities are obtained from the local region, and these might not be the same at high redshifts. However, while this conjecture would be true, it is still unlikely that the distribution of galaxy velocities at high redshifts is so different from that at low redshifts that it would lead to the bi-peak structure while the latter would not. In addition, if interpreted as the redshift caused by the proper motion of galaxies, the second component of the bi-peak structure of the distribution will correspond to a velocity as large as 3000 km s^{-1} , suggesting that, besides that at $v_{Dopp} = 0$ (corresponding to the first component), proper velocities of galaxies concentrate at $v_{Dopp} = 3000 \text{ km s}^{-1}$ as well. This interpretation, either for high or low redshifts, is obviously not acceptable.

Based on the Friedmann-Robertson-Walker cosmology, one can verify that, in a flat universe, small intervals of redshift and the radial coordinate can be related by

$$\Delta z = \frac{H_0 R_0 \Delta r}{c} \sqrt{\Omega_m (1+z)^3 + 1 - \Omega_m}, \quad (6)$$

where H_0 is the Hubble constant, R_0 is the scale factor and Ω_m is the parameter of the matter density of the universe at the present epoch.

Assigning $z_{em} - z_{abs} = \Delta z$ and taking $z_{em} = z$ we find from (1) that $\tilde{z}_{Dopp} = -\Delta z/(1+z)$. In this way we get

$$\tilde{z}_{Dopp} = -\frac{H_0 R_0 \Delta r}{c} \frac{\sqrt{\Omega_m (1+z)^3 + 1 - \Omega_m}}{1+z}. \quad (7)$$

To calculate the value of \tilde{z}_{Dopp} with (7) we adopt $H_0 = 100 h k m s^{-1} M p c^{-1}$ together with the popular values of $(\Omega_m, \Omega_\Lambda) = (0.28, 0.72)$ (Perlmutter et al. 1999) which correspond to a flat universe. Let

$$f(z) \equiv \frac{\sqrt{\Omega_m (1+z)^3 + 1 - \Omega_m}}{1+z}. \quad (8)$$

For the sample employed, emission redshifts range from 0.158 to 4.733. We find $f(0.158) = 0.928$ and $f(4.733) = 1.28$ for the adopted parameters. Therefore, $-1.28 H_0 R_0 \Delta r / c \leq \tilde{z}_{Dopp} \leq -0.928 H_0 R_0 \Delta r / c$ is maintained for this sample.

The number density of low-surface brightness galaxies with $23 < \mu_0 < 25$ V mag/arcsec² is $N = 0.01_{-0.005}^{+0.006}$ galaxies $h_{50}^3 \text{ Mpc}^{-3}$ (Dalcanton et al. 1997); then the typical distance $R_0 \Delta r$ between two neighboring galaxies is about $2.32 h^{-1} \text{ Mpc}$ (note that $1 h_{50}^3 \text{ Mpc}^{-3} = 8 h^3 \text{ Mpc}^{-3}$), which leads to $H_0 R_0 \Delta r / c \simeq 7.5 \times 10^{-4}$. Thus, for emission redshifts ranging from 0.158 to 4.733, this typical distance would correspond to the extensive Doppler redshift in the range of $-9.6 \times 10^{-4} \leq \tilde{z}_{Dopp} \leq -7.0 \times 10^{-4}$. The value of \tilde{z}_{Dopp} obtained here is far less in magnitude than the second component, $\tilde{z}_{Dopp} \simeq -0.01$. If high-surface brightness galaxies are considered, the average distance between galaxies becomes smaller than $2.32 \times h^{-1} \text{ Mpc}$, and then the situation would become worse. Therefore the assumption of the second component reflecting the average distance of galaxies can be ruled out.

The density of rich galaxy clusters is about 10^{-5} to $10^{-6} h^3 \text{ Mpc}^{-3}$ (Bahcall and Cen 1993). Then the average distance between two neighboring clusters is ~ 46.4 to $100 h^{-1} \text{ Mpc}$. Taking $R_0 \Delta r \simeq 46.4 h^{-1} \text{ Mpc}$ one obtains $H_0 R_0 \Delta r / c \simeq 0.015$, while taking $R_0 \Delta r \simeq 100 h^{-1} \text{ Mpc}$ leads to $H_0 R_0 \Delta r / c \simeq 0.032$. For emission redshifts ranging from 0.158 to 4.733, they correspond to

the extensive Doppler redshift in the ranges of $-0.019 \leq \tilde{z}_{Dopp} \leq -0.014$ and $-0.041 \leq \tilde{z}_{Dopp} \leq -0.030$, respectively. This shows that the value of \tilde{z}_{Dopp} caused by the typical distance between clusters shares the same order of magnitude of that of the second component. Hence, while the absorbers inside the same cluster as the quasar concerned could contribute to the first component, the typical distance between clusters could account for the second component. The density of galaxies in the space between clusters must be less than that within clusters, and this can account for the gap between the two peaks. Due to this gap and the two peaks, a bi-peak structure would naturally be formed.

5 Discussion and conclusions

In this section, we discuss some issues regarding the reality of the two peaks and the gap.

If the peak at $\tilde{z}_{Dopp} \simeq -0.01$ can indeed be accounted for by the average spacing between clusters, are there many peaks separated by this spacing in the distribution of the redshift? To find an answer to this, we make a power spectral analysis and find no periods existing in the distribution. In fact, the spacing between cosmological sources is not a linear function of \tilde{z}_{Dopp} when the spacing is not small enough. For a flat universe, one has

$$r_{em} - r_{abs} = \frac{c}{H_0 R_0} \int_{1+z_{abs}}^{1+z_{em}} \frac{1}{\sqrt{\Omega_M x^3 + 1 - \Omega_M}} dx. \quad (9)$$

Applying (1) we come to

$$\frac{H_0 R_0 (r_{em} - r_{abs})}{c} = \int_{(1+z_{em})(1+\tilde{z}_{Dopp})}^{1+z_{em}} \frac{1}{\sqrt{\Omega_M x^3 + 1 - \Omega_M}} dx. \quad (10)$$

According to (10), it is understandable why we do not find any periods in the distribution of \tilde{z}_{Dopp} .

Even if no periodicity in the distribution of \tilde{z}_{Dopp} is to be expected, should we have seen more than one peak in the distribution, corresponding to intervening clusters at multiples of the average cluster distance? Let us recall the fact that the gap, which is expected to represent the space between galaxies, is not detected. As explained above, this gap as well as other possible nearby gaps are entirely covered by the distribution of the proper motions of galaxies. We suspect that there might be other factors that seal other gaps between clusters. A probable factor might be the random distribution of clusters that makes the observed distance between the host galaxy of the quasar and the first absorbing cluster to vary significantly and the distribution of this distance might entirely cover the expected gaps. However, no matter how the distribution is, there will be

a lower limit of the concerned distance. (Suppose that clusters concerned here are not merging. If there are two clusters located very closely, they would be kept away from each other due to the angular momentum, otherwise they would be merged. The distance that keeps two closely located clusters away and not being merged can be regarded as that lower limit.) It would probably be this lower limit that allows the gap, which we observe in Fig. 1, to be available.

Note that the quasar sample employed comes from a catalog and is in no sense complete. Even for all these quasars, the derived sample consisting of the 1317 absorption redshifts is not complete at all. Thus, our result is not conclusive.

Because of the nature of the catalogue, the quality of the data is very heterogeneous. As the typical value of the extensive Doppler redshift we concerned is as small as -0.01 , the result might be affected by some poor data included in our analysis. Contained in our sample, there are some BAL quasars. Since these objects have absorption lines close in redshift to emission lines due to outflows related to the quasars, they may obviously affect the above distribution analysis. With this in mind, we omit 34 BAL quasars found in the 401 sources and get a subsample containing 1200 extensive Doppler redshifts. The distribution of the extensive Doppler redshift of this subsample is shown in Fig. 3. Displayed in the figure, we find that the bi-peak structure is maintained.

Though for different sources of a catalogue, as we what we employ in this paper, the absorption systems as well as the thresholds for detection of the systems might be much different, it is still possible to estimate the measurement errors according to the number of significant figure of the given value. Here, we simply assume the uncertainty of each absorption redshift provided in the catalogue is a unit of its last significant figure, which we call the first uncertainty. In addition, we consider a worse situation, taking 10 times of the first uncertainty as another uncertainty which is called the second uncertainty. For example, for an absorption redshift of 2.5167 presented in the catalogue, we take 0.0001 as its first uncertainty and 0.001 as its second uncertainty, while for that of 2.98, we take 0.01 as its first uncertainty and 0.1 as its second uncertainty.

Presented in Chaffee et al. (1988) is a $z_{abs} = 1.77642$ system for MC 1331+170. We find from Table 2 of Chaffee et al. (1988) that the observed width of the 1328.83 \AA line can be as small as 0.04 \AA . Taking the uncertainty of this line as 0.02 \AA , we get the resultant uncertainty of the absorption redshift as 0.000015. In our sample, the smallest value of the first uncertainty of the absorption redshift is 0.0001. It seems that the first uncertainty we defined above is quite

reasonable for many sources.

With the first uncertainty, we get Fig. 4, where, for the sake of comparison, the curve of Fig. 1 is also plotted. Shown in this figure, the bi-peak structure is obviously seen. While the position of the first peak remains unchanged, the range of the position of the second peak spreads mildly. With the second uncertainty we have Fig. 5. Probably due to the big uncertainties adopted, the counts spread more randomly in this figure. However, the bi-peak structure can also be seen (though being less obvious and shifted slightly, and with less counts for the two peaks). This suggests that, the main conclusion obtained above, the existence of the bi-peak structure, is not significantly affected by the measurement error of the adopted absorption redshifts.

To estimate the significance of the existence of the two peaks as well as the gap between them, we simply assume that the bi-peak structure is not true and then check if this assumption is acceptable in terms of statistics.

Suppose the peaks and the gap do not exist according to the distribution of the probability of events but result from fluctuation. One therefore can assume a monotonic function of probability in the vicinity of the gap. Theoretically, one should try all possible monotonic functions and then find out the one with the largest probability. Here, according to Fig.1, we simply assume a parabolic function of the distribution of the probability ranging from $\tilde{z}_{Dopp} = -0.0250$ to $\tilde{z}_{Dopp} = 0.0025$, covering the gap as well as the two peaks. The best fit of the data in this range yields a value of $\chi^2 = 8.40$ (where, the number of data points is 11) which corresponds to the following function of the count density: $C(\tilde{z}_{Dopp}) = -5150000\tilde{z}_{Dopp}^2 + 318000\tilde{z}_{Dopp} + 14400$, where, the integral of $C(\tilde{z}_{Dopp})$ over the range is set to be the same as the sum of the observed count within the same range. Shown in Fig. 6 are the expected counts of this curve, within the corresponding bins.

Let us study the statistical significance of the existence of the bi-peak structure in two different ways. First, we simply examine the goodness of fit of the above function with the observed counts, which can be realized by calculating the probability of the χ^2 obtained above. Here, we take the function obtained above as the null hypothesis. As the integral of $C(\tilde{z}_{Dopp})$ over the range is set to be the same as the sum of the observed count within the range and the number of data points is 11, the number of degrees of freedom is 10. The probability of exceeding the value of χ^2 obtained above for the given number of degrees of freedom is only $P\{\chi^2 = 8.40, \nu = 10\} = 0.590$, which indicates that the fit is poor.

Second, let us consider the probabilities of the occurrence of the three events: the second peak, the gap, and the first peak. Taking the function obtained above as the null hypothesis, the probability of the occurrence of the observed relative frequency of the event within a certain bin in this range would be available, which is $\int_{\tilde{z}_{Dopp,1}}^{\tilde{z}_{Dopp,2}} C(\tilde{z}_{Dopp}) d\tilde{z}_{Dopp}/n$, here $n = 1317$ is the total count concerned. From the best fit function, we get the probabilities of $p_{peak,2} = 0.0233$, $p_{gap} = 0.0266$, and $p_{peak,1} = 0.0282$ for the events of the second peak, the gap, and the first peak, respectively. One finds from Fig. 1 that the counts of the second peak, the gap, and the first peak are $n_{peak,2} = 36$, $n_{gap} = 22$, and $n_{peak,1} = 45$, respectively. We observe that, the three events are not independent. Let us redefine the three events by adjusting their relative frequencies (or the corresponding total counts) and probabilities so that they are independent. Let the relative frequency of the second peak be $n_{peak,2}/n$ and its probability be $p_{peak,2}$. Then, there are $n - n_{peak,2}$ counts left. For the gap, while its relative frequency can be taken as $n_{gap}/(n - n_{peak,2})$, its probability now becomes $p_{gap}/(1 - p_{peak,2})$. In the same way, for the first peak, while its relative frequency can be taken as $n_{peak,1}/(n - n_{peak,2} - n_{gap})$, its probability now becomes $p_{peak,1}/(1 - p_{peak,2} - p_{gap})$. The three events so defined are now independent. The probabilities of the occurrence of the three independent events can now be calculated by

$$p'_{peak,2} \equiv P\left\{\left|\frac{n_{obs}}{n} - p_{peak,2}\right| > \left|\frac{n_{peak,2}}{n} - p_{peak,2}\right|\right\}, \quad (11)$$

$$p'_{gap} \equiv P\left\{\left|\frac{n_{obs}}{n - n_{peak,2}} - \frac{p_{gap}}{1 - p_{peak,2}}\right| > \left|\frac{n_{gap}}{n - n_{peak,2}} - \frac{p_{gap}}{1 - p_{peak,2}}\right|\right\}, \quad (12)$$

and

$$\equiv P\left\{\left|\frac{n_{obs}}{n - n_{peak,2} - n_{gap}} - \frac{p_{peak,1}}{1 - p_{peak,2} - p_{gap}}\right| > \left|\frac{n_{peak,1}}{n - n_{peak,2} - n_{gap}} - \frac{p_{peak,1}}{1 - p_{peak,2} - p_{gap}}\right|\right\}, \quad (13)$$

respectively, where n_{obs} denotes the observed count within the bin concerned.

It is known that, for a certain probability p , when the total count $n \rightarrow \infty$, the distribution of the observed relative frequency n_{obs}/n would approach that of gauss, with its mean being p and its variance being $p(1 - p)/n$. Calculating with the gauss distribution, we obtain the probabilities for the occurring of the three independent events ($E_1 \equiv \{|\frac{n_{obs}}{n} - p_{peak,2}| > |\frac{n_{peak,2}}{n} - p_{peak,2}|\}$, $E_2 \equiv \{|\frac{n_{obs}}{n - n_{peak,2}} - \frac{p_{gap}}{1 - p_{peak,2}}| > |\frac{n_{gap}}{n - n_{peak,2}} - \frac{p_{gap}}{1 - p_{peak,2}}|\}$ and $E_3 \equiv \{|\frac{n_{obs}}{n - n_{peak,2} - n_{gap}} - \frac{p_{peak,1}}{1 - p_{peak,2} - p_{gap}}| > |\frac{n_{peak,1}}{n - n_{peak,2} - n_{gap}} - \frac{p_{peak,1}}{1 - p_{peak,2} - p_{gap}}|\}$): $p'_{peak,2} = 0.324$ for E_1 , $p'_{gap} = 0.0261$ for E_2 , and $p'_{peak,1} = 0.199$ for E_3 , respectively. The probability of none of the three events occurring is $(1 - p'_{peak,2})(1 - p'_{gap})(1 - p'_{peak,1}) = 0.527$ (the events of E_1 , E_2 and E_3 not occurring). The probabilities of one of

the three events occurring but the other two not occurring are $p'_{peak,2}(1-p'_{gap})(1-p'_{peak,1}) = 0.253$ (the event of E_1 occurring but the events of E_2 and E_3 not occurring), $(1-p'_{peak,2})p'_{gap}(1-p'_{peak,1}) = 0.0141$ (the event of E_2 occurring but the events of E_1 and E_3 not occurring), and $(1-p'_{peak,2})(1-p'_{gap})p'_{peak,1} = 0.131$ (the event of E_3 occurring but the events of E_1 and E_2 not occurring). The probabilities of two of the three events occurring but the other one not occurring are $p'_{peak,2}p'_{gap}(1-p'_{peak,1}) = 0.00677$ (the events of E_1 and E_2 occurring but the event of E_3 not occurring), $p'_{peak,2}(1-p'_{gap})p'_{peak,1} = 0.0628$ (the events of E_1 and E_3 occurring but the event of E_2 not occurring), and $(1-p'_{peak,2})p'_{gap}p'_{peak,1} = 0.00351$ (the events of E_2 and E_3 occurring but the event of E_1 not occurring). The probability of all the three events occurring is $p'_{peak,2}p'_{gap}p'_{peak,1} = 0.00168$ (the events of E_1 , E_2 and E_3 occurring). The observational fact is that all the three events (E_1 , E_2 and E_3) occur. Thus, the null hypothesis is not acceptable. In views of statistics, the existence of the bi-peak structure is significant.

To find out if the bi-peak structure is stable, let us examine the distribution of the extensive Doppler redshift with subsamples. One should notice that the largest value of counts in Fig. 1 is 45. This suggests that subsamples selected should not be much smaller than the total sample. We hence select a subsample with 200 sources out of the 401 source sample. The selection is made with the method of random sampling and we obtain a 200 source sample with 655 absorption redshifts. We therefore have 655 extensive Doppler redshifts. The distribution of \tilde{z}_{Dopp} of this subsample is shown in Fig. 7. We find from the figure that the bi-peak structure is still observable. In the same way, we get the best fit parabolic function of the distribution of the probability, ranging from $\tilde{z}_{Dopp} = -0.0250$ to $\tilde{z}_{Dopp} = 0.0025$, as $C(\tilde{z}_{Dopp}) = -8980000\tilde{z}_{Dopp}^2 - 1.02\tilde{z}_{Dopp} + 6610$. The fit yields $\chi^2 = 9.54$ (where, the number of data points is 11). For the same reason, the number of degrees of freedom is taken to be 10. The probability of exceeding the value of χ^2 obtained above for the given number of degrees of freedom is only $P\{\chi^2 = 9.54, \nu = 10\} = 0.482$, which indicates that the fit is poor. Also in the same way, we redefine the three events (the second peak, the gap, and the first peak) to make them independent. Then we get the probabilities of the three independent events ($p'_{peak,2} = 0.262$, $p'_{gap} = 0.0187$, $p'_{peak,1} = 0.397$) and the product of them, which is $P = 0.00195$. It shows that the existence of the bi-peak structure is significant as well with this subsample. When selecting a smaller subsample (a 100 source sample with 345 absorption redshifts), we find that the bi-peak structure is poorly detectable. We come to the conclusion that

the bi-peak structure is detectable as long as the sample employed is large enough.

Besides the distribution of the extensive Doppler redshift, can one find any other signs of the clustering in the distribution of other redshifts? As the extensive Doppler redshift is defined with both absorption and emission redshifts, we wonder if the distribution of absorption or emission redshifts individually show some signs of clustering. Shown in Fig. 8 are the distributions of the absorption and emission redshifts of the 401 source sample. We do not find any signs of the clustering in this figure. In fact, any peaks shown in the two distributions would not be able to reveal a clustering. For example, for a peak appearing in the distribution of absorption redshifts, only a fraction of all the redshifts within the bin, which is associated with slightly larger emission redshifts, can be attributed to the second peak in Fig. 1, and the two distributions themselves (or a combination of them) cannot tell how large this fraction is.

As mentioned above, the number of absorption lines one expects along a line of sight to a quasar is given by the product of the number density of absorbers, the absorption cross-section and the path length. Absorber properties are expected to change with redshift and one can study the development of the properties with this number. However, the changes of either the number density or the absorption cross-section are unlikely to ensure that the less populated space between clusters could provide sufficient absorbers that can affect the bi-peak structure of the distribution, while possibly, they could affect the distribution of large \tilde{z}_{Dopp} which corresponds to large distances. Compared with this approach, the distribution analysis adopted in this paper refers to a different quantity, the extensive Doppler redshift (which is a relative absorption redshift defined relative to the corresponding emission redshift). The analysis is also able to draw some useful cosmological information. For example, when several samples with different emission redshifts are available, one can determine the development of the distance between clusters and then can constrain the cosmological model.

Acknowledgments

It is our great pleasure to thank Dr. A. Kembhavi for his helpful suggestions. This work was supported by the Special Funds for Major State Basic Research Projects (“973”) and National Natural Science Foundation of China (No. 10273019).

REFERENCES

- Bahcall, N.A. and Cen, R. 1993, ApJ, 407, L49
- Chaffee, Jr., F. H., Black, J. H., and Foltz, C. B. 1988, ApJ, 335, 584
- Dalcanton, J. J. et al, 1997, ApJ, 114, 635
- Gaskell, C. M. 1982, ApJ, 263, 79
- Hewitt, A. and Burbidge, G. 1993, ApJS, 87, 451
- Junkkarinen, V., Hewitt, A. and Burbidge, G. 1991, ApJS, 77, 203
- Kembhavi, A. K. and Narlikar, J. V. 1999, in Quasars and Active Galactic Nuclei, (Cambridge: Cambridge University Press)
- Perlmutter, S., et al. 1999, ApJ, 517, 565
- Peterson, B. M. 1997, in An Introduction to Active Galactic Nuclei, (Cambridge: Cambridge University Press)
- Qin, Y.-P., Xie, G.-Z., Zheng, X.-T., and Liang, E.-W. 2000, astro-ph/0005006
- Sargent, W. L. W., Boksenberg, A., and Steidel, C. C. 1988, ApJS, 68, 539
- Tytler, D. 1982, Nature, 298, 427
- Weymann, R. J., Carswell, R. F., and Smith, M. G. 1981, ARA&A, 19, 41
- Weymann, R. J., Willams, R. E., Beaver, E. A., and Miller, J. S. 1977, ApJ, 213, 619
- Willick, J. A., Courteau, S., Faber, S. M., et al. 1997, ApJS, 109, 333

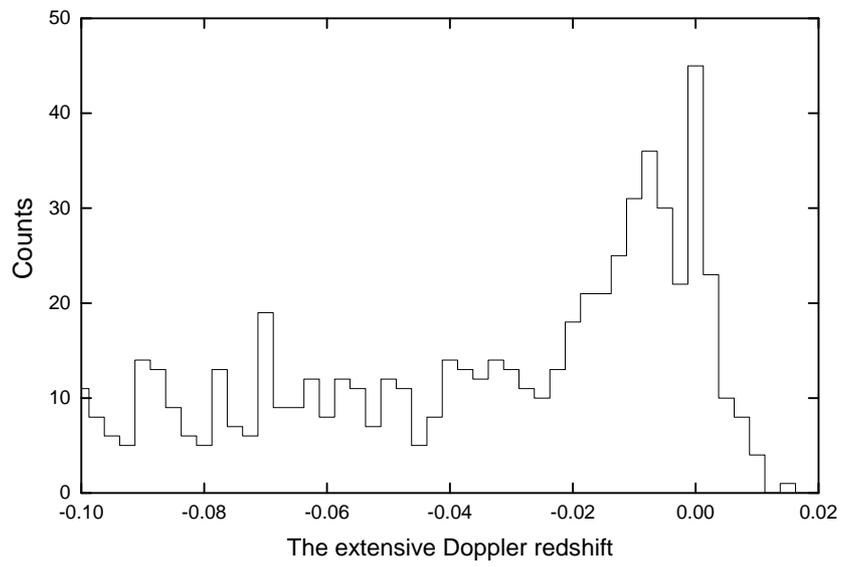


Figure 1: The distribution of the 1317 extensive Doppler redshifts available from a sample of 401 quasars, where only the main part (from -0.10 to 0.02) of the distribution is plotted.

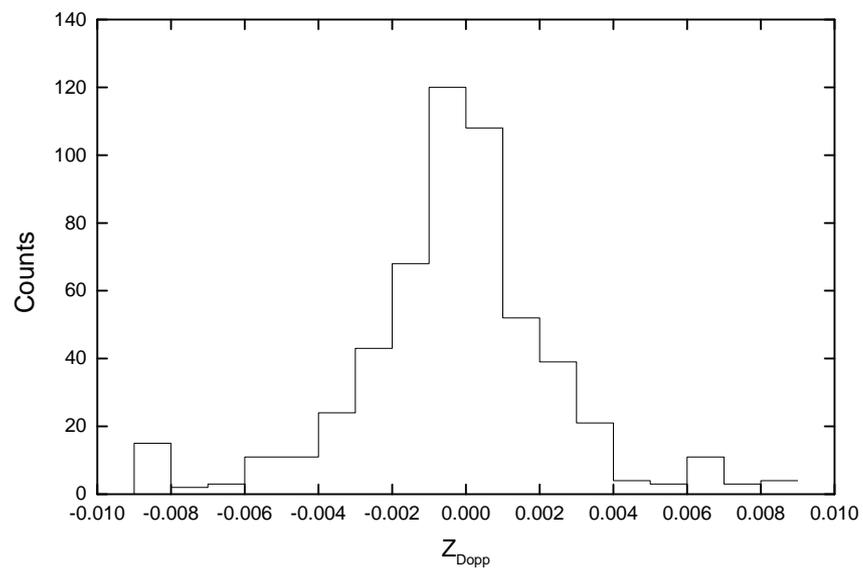


Figure 2: The distribution of Doppler redshifts derived from the proper velocities of galaxies, where the number in total is 544.

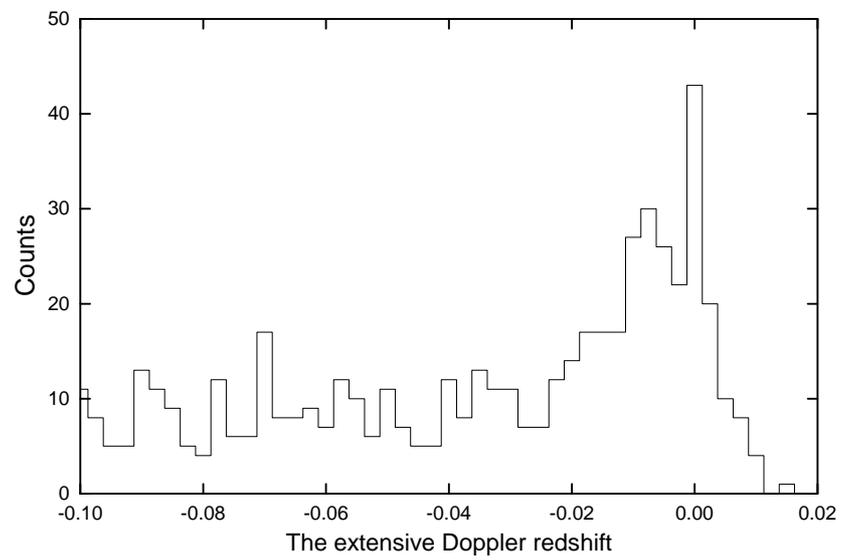


Figure 3: The distribution of the extensive Doppler redshift of the subsample that omits the 34 BAL quasars.

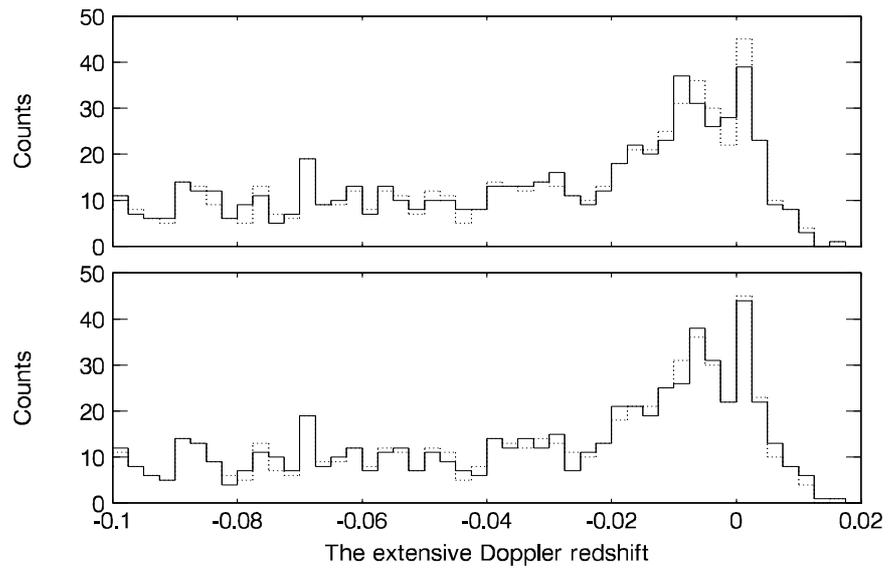


Figure 4: The distribution of the extensive Doppler redshift of the 401 source sample with the extensive Doppler redshift derived from the absorption redshifts minus or plus the first uncertainty. The upper panel corresponds to the case of the absorption redshift minus the first uncertainty (the solid line), while the lower panel represents the case of the absorption redshift plus the first uncertainty (the solid line). In both panels, the curve in Fig. 1 is also plotted (the dotted line).

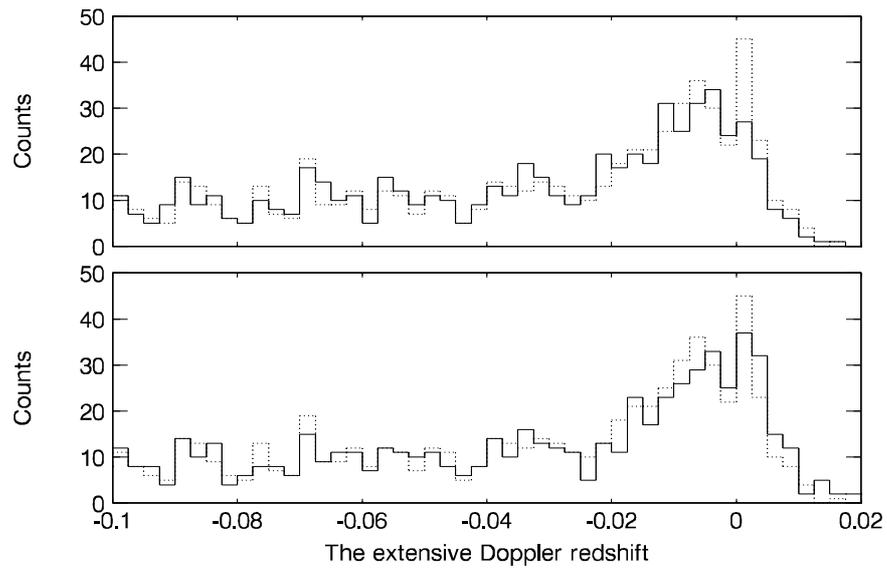


Figure 5: The distribution of the extensive Doppler redshift of the 401 source sample with the extensive Doppler redshift derived from the absorption redshifts minus or plus the second uncertainty. The upper panel corresponds to the case of the absorption redshift minus the second uncertainty (the solid line), while the lower panel represents the case of the absorption redshift plus the second uncertainty (the solid line). In both panels, the curve in Fig. 1 is also plotted (the dotted line).

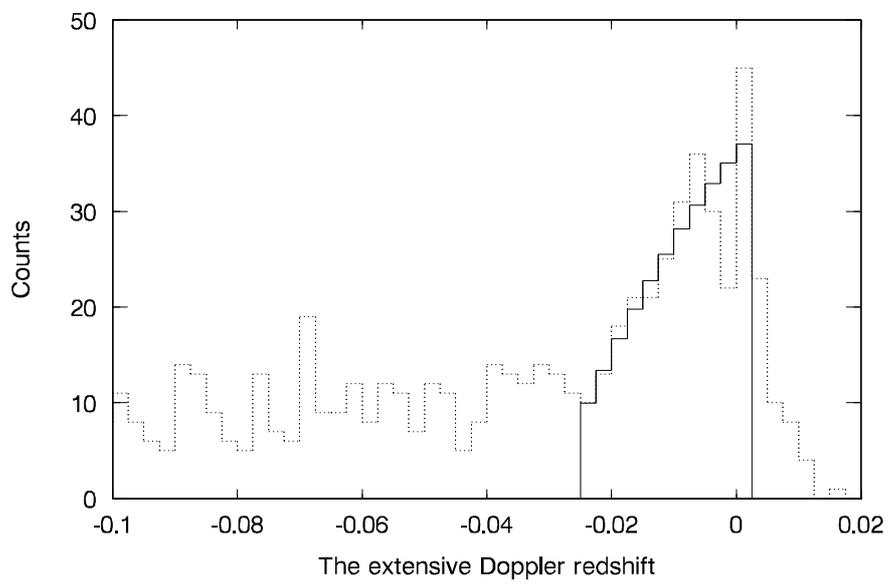


Figure 6: The expected counts of the best fit parabolic curve (the solid line) of the 401 source sample, in the vicinity of the gap, where the curve in Fig. 1 is also plotted (the dotted line).

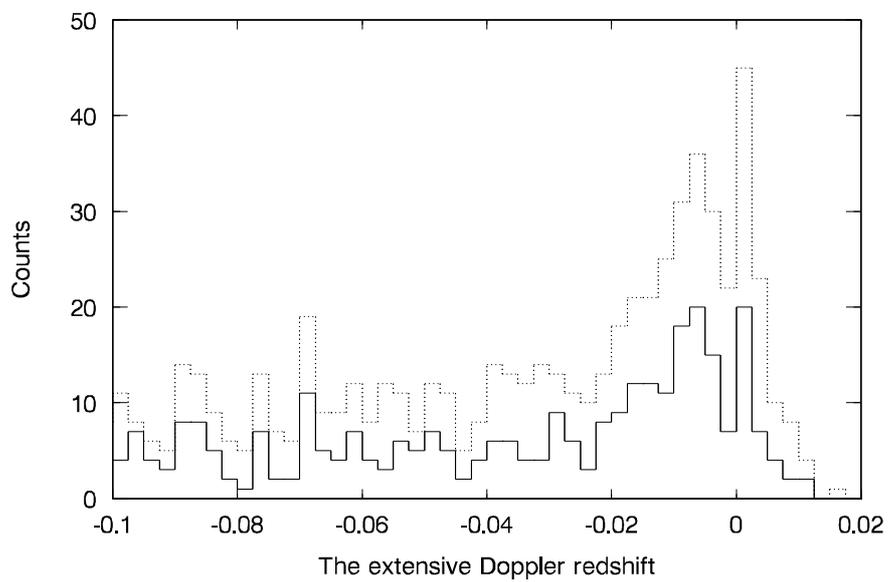


Figure 7: The distribution of the extensive Doppler redshift of the 200 source subsample (the solid line), where the curve in Fig. 1 is also plotted (the dotted line).

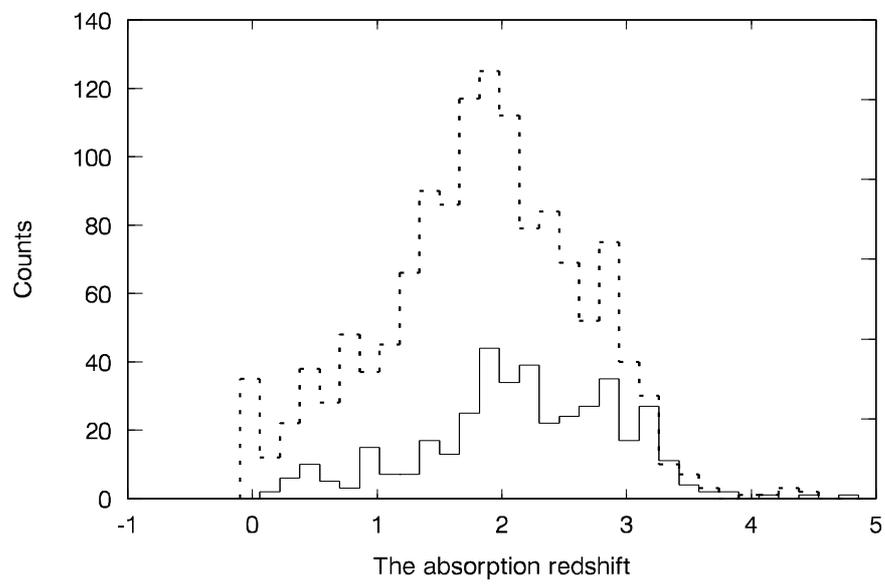


Figure 8: The distributions of the 401 emission redshifts (the solid line) and the 1317 absorption redshifts (the dotted line).